Global Structure of Three-Way DNA Junctions with and without Additional Unpaired Bases: A Fluorescence Resonance Energy Transfer Analysis†

Frank Stühmeier,‡ Jonathan B. Welch,§ Alastair I. H. Murchie,§ David M. J. Lilley,§ and Robert M. Clegg*,‡

Max-Planck-Institut für biophysikalische Chemie, Abteilung Molekulare Biologie, Am Fassberg 11, D-37077 Göttingen, Germany, and Cancer Research Campaign Nucleic Acid Structure Research Group, Department of Biochemistry, The University, Dundee DD1 4HN, United Kingdom

Received February 3, 1997; Revised Manuscript Received July 11, 1997⊗

ABSTRACT: The structure of three-way DNA junctions with and without extrahelical adenine nucleotides in one strand at the branch point of the junction (i.e., A_n bulges with $n = 0$, 1, 2, and 3) has been investigated by fluorescence resonance energy transfer. The structure of the junction without bulged nucleotides was found to have a symmetric trigonal geometry. With bulges, the arrangement of the arms becomes asymmetrical. The energy transfer results suggest a model of bulged junctions where the angle between two of the arms is significantly smaller than between the other two pairs of arms. The acute angle becomes smaller as the number of nucleotides in the bulge increases. The FRET efficiencies of the junctions are the same in the presence of Mg^{++} and Na^{+} ions.

The geometrical structures of branched nucleic acid molecules and the effect of a branch point on the thermodynamic stability and dynamics of these molecules have been studied in detail in the last few years (Altona et al., 1996; Lilley & Clegg, 1993a,b; Seeman & Kallenbach, 1994). Many of these branched molecular structures, such as the four- and three-way junctions and bulged duplexes, correspond to important biological structures. The main biological relevance of branched DNA species lies in their proposed role as possible intermediates in molecular rearrangements, repair, and recombination. The branched molecules often form various characteristic structures compatible with free energy constraints that vary by changing the environmental conditions. Because the global structures of these molecules in solution are sensitive to the solvent environment, it is imperative to use experimental methods for determining their structures that can be applied in solution under a wide variety of conditions. Fluorescence resonance energy transfer (FRET)[1] has proved to be a powerful technique for investigating the structures of DNA/RNA molecules, especially when applied to a set of identical branched structures with dyes attached to different permuted positions (Clegg et al., 1992, 1994; Cooper & Hagerman, 1990; Eis & Millar, 1993; Millar, 1996; Murchie et al., 1989; Tuschl et al., 1994) or to a series of DNA molecules which differ by a local structural change (Jares-Erijman & Jovin, 1996), by a different number of base-pairs (Clegg et al., 1993) or by the presence of a bulge (Gohlke et al., 1994).

We have previously investigated the structure and thermodynamic behavior of several branched and otherwise modified DNA and RNA structures with fluorescence spectroscopic methods (Clegg et al., 1992, 1994; Gohlke et al., 1994; Murchie et al., 1989) and with comparative gel electrophoresis experiments (Bhattacharyya & Lilley, 1989; Bhattacharyya et al., 1990; Duckett et al., 1988, 1990, 1995a; Pöhler et al., 1994; Welch et al., 1993; Welch et al., 1995). It has been proved to be especially useful to compare the FRET results to similar experiments carried out by electrophoresis (Lilley & Clegg, 1993b). These studies of branched and nonlinear DNA and RNA structures have provided insight into the folding behavior of these molecules under various experimental conditions. The configuration of branched nucleic acid junctions depends on the balance between various energetic interactions at the point of branch exchange, such as stacking interactions between bases in neighboring arms and electrostatic and steric repulsions between neighboring helices of branched molecules. The thermodynamic balance between these terms prescribes the most probable stereochemical arrangement of the arms at the junction of a branched structure. The relative strengths of these competing forces are affected by the ionic strength of the solution and the presence of strongly interacting ions. Several proteins interact selectively at the point of branch exchange (Bennett & West, 1995; Bhattacharyya et al., 1991; Bianchi et al., 1989, 1992; Duckett et al., 1992, 1995a; Eggleston & West, 1996; Parsons et al., 1995; Teo et al., 1995), and it appears to be a general phenomenon that the binding of proteins may produce a distortion of the branched DNA structures (Bennett & West, 1995; Duckett et al., 1995a; Parsons et al., 1995; Pöhler et al., 1996; White & Lilley, 1996).

A major factor governing the folded configuration of branched structures seems to be stacking between the end base pairs of two of the neighboring helical arms that converge at the center of the junction at the branch point. The formation of quasi-continuous helices between neigh-

† D.M.J.L. thanks the CRC for financial support and R.M.C. and D.M.J.L. thank the British Council-DAAD for a travel grant. F.S. and R.M.C. thank the Deutsche Forschungsgemeinschaft for financial support: DFG-Project Nr. II B 2 C1 84/2-2.

* Author to whom correspondence should be addressed.

‡ Max-Planck-Institut für biophysikalische Chemie.

§ The University.

⊗ Abstract published in *Advance ACS Abstracts,* September 15, 1997.

[1] Abbreviations: FRET, fluorescence resonance energy transfer; TMRh, tetramethylrhodamine; NMR, nuclear magnetic resonance; TB, Tris borate buffer.

S0006-2960(97)00244-4 CCC: $14.00

boring arms by helix−helix stacking has been proposed to play a central role in the folded structure when the solution conditions and the steric constraints allow it (Duckett et al., 1988; Leontis et al., 1994).

For three-way DNA junctions with full base pairing and no bulged nucleotides, 3H, a folded structure with coaxial stacking of two of the helices is sterically not possible unless one or more base pairs at the branch point are abolished, or distorted.[2] Electrophoretic studies of some 3H junctions without bulges indicate that the helical arms are all extended at equal angles to each other even in the presence of magnesium ions and that the thymine bases at the point of strand exchange are reactive to osmium tetroxide (Duckett & Lilley, 1990). NMR experiments also show that the helical arms of three-way junctions without bulges do not stack on each other (Leontis et al., 1993; Rosen & Patel, 1993a; Zhong et al., 1994).

The inclusion of bulges at the point of branch exchange has also a major effect on the relative orientation of the arms at higher ionic strength. The structures of bulged three-way junction molecules ($3HS_n$) have been investigated by comparative gel electrophoresis and NMR, and some general distinguishing structural characteristics of three-way junctions can be surmised from these data. It has been shown that unpaired bases at the point of branch exchange change the electrophoresis pattern of a series of three-way junction molecules with arms of different lengths; the molecules seem to fold into well-defined structures in the presence of sufficient metal ions (Leontis et al., 1993; Welch et al., 1993). The folded structure can be explained if it is assumed that the arm that contains both DNA strands without extra nucleotides coaxially stacks with one of the other two arms (Welch et al., 1993); the most acute angle between any two arms is between the third (nonstacked) arm and one of the two coaxially stacked arms. The unstacked arm is inclined away from the bulge, and the extent of inclination depends on the size of the bulge. The NMR studies have shown directly that the presence of unpaired bases in one strand at the point of branch exchange mediates an interaction between two of the three arms (stacking of the two helical arms at the branch point) while the third helix is unstacked and its helical axis extends away from the point of strand exchange (Ouporov & Leontis, 1995; Overmars et al., 1996; Rosen et al., 1992; Rosen & Patel, 1993b; Welch et al., 1993). Later it was shown that the choice of stacking partners is sequence dependent (Welch et al., 1995), generating two stereochemically inequivalent conformers. The conclusion is that the overall conformation of the bulged three-way junction is not only salt dependent, but also depends on the nucleotide sequence at the branch point.

In this paper, we have applied FRET in order to investigate the structure of the three-way junction in solution in order to determine the influence of up to three unpaired adenine bases on the global orientations of the arms. The central sequences correspond to the junction I that has been previously investigated by comparative gel electrophoresis (Welch et al., 1993, 1995).

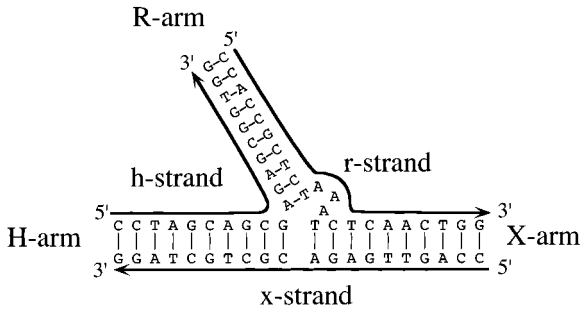

FIGURE 1: The sequence of the $3HS_3$ junction: a three-way junction with three unpaired adenine nucleotides at the point of the strand exchange. The arms are labeled H, R, and X and the single strands are labeled h, r, and x. The 5 → 3′ direction of the strands is indicated by the arrows. In each doubly labeled vector, the donor and acceptor are covalently attached to the 5′ ends of two of the three strands in each three-way junction molecule. The geometry corresponds to a two-dimensional structure that we propose for the $3HS_3$ molecule.

MATERIALS AND METHODS

Synthesis and Purification of Oligonucleotides. Oligonucleotides were synthesized using β-cyanoethylphosphoramidite chemistry (Beaucage & Caruthers, 1981; Sinha et al., 1984) implemented on a 394 DNA synthesizer (Applied Biosystems). Amino groups at the end of six-carbon linkers were introduced at the 5′ end of the DNA strands by a final coupling step with *N*-methoxytrityl-2-aminohexyl-2-cyanoethyl-*N*,*N*-diisopropylaminophosphite (Connolly, 1987). Fully deprotected oligonucleotides were ethanol precipitated and purified by HPLC on a 4000A DEAE weak anion exchange column (Nucleogen) followed by a C8 reverse phase column (Aquapore). Pure oligonucleotides eluted as a sharp peak. Peak fractions were reduced in volume and then ethanol precipitated. The six-carbon linkers were chosen to give the fluorescein sufficient rotational freedom, and so that the TMRh fluorescence characteristics and conformers of dye-DNA correspond to those of an earlier study (Vámosi et al., 1996).

Conjugation with Fluorescent Dyes. Oligonucleotides were conjugated with fluorescein in a final coupling step on the DNA synthesizer using the fluorescein phosphoramidite (Applied Biosystems). The succinimidyl ester of 5-carboxytetramethylrhodamine TMRh (Molecular Probes) was attached to the 5′ amino linker as described before (Clegg et al., 1992). Unreacted dyes were removed by chromatography on Sephadex G25 (Pharmacia). Unreacted oligonucleotides were separated from the oligonucleotides conjugated with dye by 20% PAGE in 90 mM Tris borate (pH 8.3) and 7 M urea. The terminal two base pairs were kept constant for all arms of the molecules to ensure the same molecular environment for the dyes.

Construction of the Fluorescently Labeled Three-Way Junctions. The following oligonucleotides were synthesized (see Figure 1 for the notation of the arms and the strands of the $3HS_n$ molecules):

[2] The notation of branched nucleic acid structures proposed by Lilley et al. (1995) will be used in the text. For the three way junctions $3HS_n$ means three helical arms meeting at a branch point and a single stranded loop of *n* nucleotides on one of the strands. 3H refers to a three-way junction without a bulge (only three helices). In addition, in this paper we identify the strand (h, r or x) that is labeled with either TMRh (R) or fluorescein (F) in parenthesis following this notation; for instance $3HS_2$(rRxF) stands for a three-way junction with a two nucleotide bulge where the r-strand is labeled by TMRh and the x-strand is labeled with fluorescein.

h-strand: 5′ CCT AGC AGC GAG AGC GGT GG 3′

x-strand: 5′ CCA GTT GAG ACG CTG CTA GG 3′

r-strand s0: 5′ CCA CCG CTC T TC TCA ACT GG 3′

r-strand s1: 5′ CCA CCG CTC TA TC TCA ACT GG 3′

r-strand s2:
5′ CCA CCG CTC TAA TC TCA ACT GG 3′

r-strand s3:
5′ CCA CCG CTC TAAATC TCA ACT GG 3′

The central sequences used in this study (i.e., all nucleotides other than the outer two at the 3′ and 5′ ends) are identical to the sequences of the central bases of junction I used in an earlier study (Welch et al., 1993). Complementary combinations of fluorescein- and TMRh-conjugated oligonucleotides were hybridized in 90 mM Tris borate (pH 8.3) in the presence of 50 mM NaCl and 2 mM $MgCl_2$ by slow cooling from 80 to 0 °C. The junctions were purified by 20% native polyacrylamide gel electrophoresis. The samples were recovered by high-salt electroelution.

Preparation of the DNA Samples for Spectroscopic Measurements. The DNA samples were first dialyzed into 90 mM Tris borate (pH 8.3), 100 mM NaCl, and 0.5 mM EDTA and finally dialyzed twice into the same buffer without EDTA. Absorption measurements were made on these solutions from 240 to 640 nm to determine the concentration of the samples and to control the extent and the quantity of the labeling. The maximum absorption peaks of the dyes (from 450 to 600 nm) are well removed from the absorption of the DNA (260 nm). The absorption of TMRh (the energy acceptor) at its maximum can be measured without interference from fluorescein (the energy donor). The overlapping contribution by the acceptor to the spectral region where the donor absorbs can be subtracted from the total absorbance spectrum; this yields the donor absorbance at the wavelength of the maximum donor absorption. All spectroscopic measurements were carried out at 4 °C.

Spectroscopic Equipment. Absorption measurements were taken on a UVICON 820 spectrophotometer (Kontron, Zürich). Steady-state fluorescence spectra and anisotropy measurements were made with an SLM 8000S instrument (SLM Aminco, Rochester). The spectral measurements were corrected for lamp fluctuations and wavelength dependence of the emission channel. Polarization artifacts were avoided by using "magic angle" conditions (Lakowicz, 1983; Nickel, 1989). The spectra were required and processed using the program Lab View (National Instruments, Austin) implemented on Macintosh computers (Apple, Cupertino). The fluorescence spectra for FRET were collected over a broad range of emission wavelengths ($\lambda_{ex} = 490$ nm, $\lambda_{em} = 500-650$ nm for the FRET spectrum, and $\lambda_{em} = 560$ nm and $\lambda_{ex} = 570-650$ nm for the acceptor spectrum). Fluorescence anisotropies r were calculated from measurements of polarized fluorescence intensities F according to the expression $r = (F_{0/0} - GF_{0/90})/(F_{0/0} + 2GF_{0/90})$, with $G = (F_{90/0}/F_{90/90})$ (Jablonski, 1957; Lakowicz, 1983).[3] Fluorescence spectral and anisotropy measurements were corrected for the buffer signal. Measurements were performed on diluted solutions to avoid inner-filter effects or significant absorption of the excitation light in the cuvette. The fluorescence and absorption spectra of molecules labeled with donor or acceptor alone were used to decompose the spectra of the doubly labeled samples into donor and acceptor components (see below).

Determination of the Quantum Yield of TMRh. The quantum yield of TMRh covalently attached to the 5′ end of double-stranded DNA was determined for three samples by comparing the fluorescence of the samples to a fluorescence standard (Demas & Crosby, 1971) of known quantum yield (Rhodamin 101) as described before (Vámosi et al., 1996). Emission spectra were collected from 570 to 700 nm ($\lambda_{ex} = 560$ nm) and from 550 to 600 nm ($\lambda_{ex} = 540$ nm). The quantum yields were calculated using the data acquired with $\lambda_{ex} = 560$ nm; the spectral region from 560 to 570 nm was included in the integral over the total emission spectrum (which is needed for the quantum yield determination) by fitting the data from 570 to 600 nm to the emission spectra which were acquired (over the range from 550 to 600 nm) using $\lambda_{ex} = 540$ nm. The relative quantum yields were obtained from the integrated emission spectra from 560 to 700 nm.

FRET. The rate of radiationless dipole−dipole FRET from a donor (fluorescein) to an acceptor (TMRh) is given by $k_T = (R_0/R)^6/\tau_D$, where τ_D is the fluorescence lifetime of D in the absence of A, and R is the scalar donor−acceptor separation. R_0 is a constant depending on the lifetime of the donor in the absence of the acceptor, the spectral overlap of the dyes, the quantum yield of the donor, and the orientation of the transition dipole moments of the dyes (Clegg, 1996; Förster, 1948; Van Der Meer et al., 1994). The efficiency of energy transfer of a single donor−acceptor pair at a certain distance can be expressed as $E = 1/[1 + (R/R_0)^6]$. For complete rapid randomization of the relative orientations between D and A, the factor relating the orientation between the two transition dipoles, κ^2, is assumed to be $^2/_3$ (Förster, 1949).[4] The low anisotropy of the DNA samples containing fluorescein implies that this is a good assumption for this study (Clegg et al., 1992), so that for any D-A pair E is sensitive only to the scalar D-A distance.

Data Analysis. The FRET efficiencies were determined by measuring the intensity of the sensitized emission of the acceptor normalized to the fluorescence of the acceptor alone (Clegg, 1992). The intensity of the TMRh emission increases in the presence of FRET, and the intensity of the fluorescein emission correspondingly decreases. The spectral dispersion of the fluorescence intensities of the emission spectra $F(\lambda_{em}, 490)$ (excited at 490 nm, where both D and A absorb) are fitted to the weighted sum of two spectral components: (1) a standard spectrum of a three-way junction labeled only with donor $F^D(\lambda_{em}, 490)$ and (2) the fluorescence spectrum of the sample $F(\lambda_{em}, 560)$ excited at 560 nm, where only TMRh absorbs.

[3] The subscripts in this equation refer to the positions of the polarizers: 0 means the vertical position and 90 means the horizontal position; the symbol before the slash is the orientation of the excitation polarizer; the symbol after the slash is the orientation of the emission polarizer.

[4] It should be noted that for κ^2 to be $^2/_3$ it is not necessary that the conditions of rapid orientation hold. This value of κ^2 is possible even between two absolutely rigid dipoles (Clegg, 1996; Dale & Eisinger, 1974). $\kappa^2 = {}^2/_3$ is a good approximation for many cases of only partial orientational freedom (Clegg, 1996).

$$F(\lambda_{em}, 490) = aF^{D}(\lambda_{em}, 490) + (\text{ratio})_A F(\lambda_{em}, 560) \quad (1)$$

a and $(\text{ratio})_A$ are the weighting factors for the two spectral components that are fitted in the regression analysis. The fit of the data according to eq 1 is made over $\lambda_{em} = 500-540$ nm (where only D emits) and $\lambda_{em} = 570-650$ nm, where both D and A emit. $(\text{ratio})_A$ is the acceptor fluorescence signal of the FRET measurements normalized by $F(\lambda_{em}, 560)$ as shown in eq 2 (Clegg, 1992; Clegg et al., 1992):

$$(\text{ratio})_A = \frac{F(\lambda_{em}, 490) - aF^{D}(\lambda_{em}, 490)}{F(\lambda_{em}, 560)} = Ed^{+}\frac{\epsilon^{D}(490)}{\epsilon^{A}(560)} + \frac{\epsilon^{A}(490)}{\epsilon^{A}(560)} \quad (2)$$

$(\text{ratio})_A$ is linearly dependent on the efficiency of energy transfer E. It normalizes the measured sensitized FRET signal for the concentration and for the apparent quantum yield[5] of the acceptor and accounts for errors in the percentage of acceptor labeling. d^{+} is the fraction of labeling with donor molecules. The spectroscopic measurements have shown that all molecules used for the determination of the FRET efficiency were 100% labeled with donor and acceptor dye. ϵ^{D} and ϵ^{A} are the molar absorption coefficients of D and A at a given wavelength. $\epsilon^{D}(490)/\epsilon^{A}(560)$ and $\epsilon^{A}(490)/\epsilon^{A}(560)$ were determined from the absorbance spectra of the doubly labeled molecules and the excitation spectra of singly TMRh-labeled molecules.

RESULTS

Spectral Characteristics of the Dye-Labeled Three-Way Junctions. The procedures used to prepare the dye-labeled DNA molecules were designed to ensure at least uniform labeling of the DNA molecules with fluorescein and TMRh (Clegg et al., 1992). The consistency of labeling was checked spectroscopically by comparing the absorbencies of the dyes in the visible region relative to each other and relative to the absorbency of the DNA in the UV region (Clegg et al., 1994). The $(\epsilon^{dye})_{max}/(\epsilon^{DNA})_{max}$ values were constant within the error of the measurement for all the molecules, and the values indicated virtually 100% labeling for all the samples used in this study. The $\epsilon^{D}(490)/\epsilon^{A}(560)$ values were slightly different for the two series of samples used in this study because of different isomer compositions of the two TMRh-succinimidyl ester batches. We evaluated an $\epsilon^{D}(490)/\epsilon^{A}(560)$ value of 0.71 ($\pm$0.02) for the 3H samples and the samples $3HS_2$(rRxF) and $3HS_3$(hRxF) (series 1) and a values of 0.80 ($\pm$0.03) for all the other samples (series 2). The $\epsilon^{A}(490)/\epsilon^{A}(560)$ value was determined with the excitation spectra of several singly labeled TMRh samples and has a value of 0.095 ($\pm$0.002). Both $\epsilon^{D}(490)/\epsilon^{A}(560)$ and $\epsilon^{A}(490)/\epsilon^{A}(560)$ are used to calculate the efficiency of energy transfer from the $(\text{ratio})_A$ values (see eq 2). The fluorescence of fluorescein, excited at 490 nm, emits with a maximum of 518 nm, while the maximum of the TMRh fluorescence, excited at 560 nm, lies at 584 nm for the series 1 and at 586 nm for the series 2.

The measured apparent quantum yield of TMRh at 4 °C in TB buffer and 100 mM NaCl was determined for the samples $3HS_3$(hRrF), $3HS_3$(hFrR), and $3HS_2$(rFxR). The quantum yields of all double-stranded samples at this temperature are 0.20 ($\pm$0.01) for all three samples; this is in good agreement with earlier measurements from our laboratory (Vámosi et al., 1996).

The fluorescence anisotropy of each dye can be measured separately even in doubly labeled samples. At 4 °C the TMRh anisotropy is 0.260 $\pm$ 0.003 for the 3H samples and 0.270 $\pm$ 0.003 for the $3HS_2$ and $3HS_3$ samples. The anisotropy of the fluorescein [$r(518/490) \approx 0.1-0.14$] varies depending upon the extent of energy transfer (Clegg et al., 1992) and is much lower than the anisotropy of TMRh. Both dyes have similar fluorescence lifetimes, so that fluorescein must rotate considerably faster than TMRh (Clegg et al., 1992). The low anisotropy of fluorescein indicates that it is not oriented in a preferred static orientation relative to the DNA, but rotates rapidly relative to the DNA helix. These values are in good agreement with earlier studies from our laboratory (Clegg et al., 1992; Gohlke et al., 1994) and indicate the absence of free TMRh or of TMRh labeled single strands which would lead to significantly lower anisotropy values.

FRET Efficiencies of the DNA Three-Way Junction without a Bulge (3H) at 100 mM NaCl. The FRET efficiencies for all 3H molecules are approximately equal for all samples as determined from $(\text{ratio})_A$ (Table 1 and Figure 3). The FRET efficiencies for the RX and the HR vectors ($\sim$0.22) are slightly higher than the value for the HX vector ($\sim$0.20), indicating that the angle between the H and X arms may be larger than the angle between the H and R arms and between the R and X arms. However, this small difference, even though accurate and reproducible, could be due to an effect of the molecular geometry other than simply the angle between the arms.

Influence of the Bulges at the Point of Branch Exchange of the $3HS_n$ Molecule on the FRET Efficiencies at 100 mM NaCl. The FRET efficiencies for the HX vectors decrease from $\sim$0.20 to $\sim$0.16 as the number of nucleotides in the bulge at the point of strand exchange increases; for the RX vectors, the values vary only from $\sim$0.22 to $\sim$0.19 (Table 1 and Figure 3). The influence of the number of nucleotides in the bulge on the energy transfer efficiencies is more pronounced for the HX than for the RX vector; however, the energy transfer efficiencies of both the HX and the RX vector do not depend strongly on the number of unpaired nucleotides at the point of branch exchange. On the other hand, we observe a large increase in the FRET efficiency for the HR vector as the number of nucleotides in the bulge increases. For the HR vector, the FRET efficiencies for the $3HS_2$ ($E = 0.36$) and $3HS_3$ ($E = 0.48$) molecules are significantly higher than for the 3H ($E = 0.22$) molecules.

Influence of Mg^{2+} Ions on the FRET Efficiencies of the $3HS_2$ and $3HS_3$ Molecules. The FRET efficiencies of the $3HS_2$ and $3HS_3$ molecules have also been determined in 5

[5] Throughout the text we will use the term "apparent quantum yield" when referring to relative measured fluorescence intensities of samples which are excited with light of the same intensity. The true quantum yield of a fluorescent molecular species is a measure of the number of quanta emitted relative to the number of photons absorbed, and is a term which can only be used when referring to one single fluorescent species; however, if there are multiple fluorescing species in solution, which may even interconvert, we can only measure parameters related to an apparent quantum yield of the mixture in a steady-state fluorescence measurement. In addition, it could be that samples being compared have different absorption coefficients, and then, even if the samples are composed of single chromophore species, the ratio of their fluorescence intensities is not the ratio of their quantum yields.

Table 1: $(ratio)_A$ and Efficiency Values for the Different Labeling Vectors with Na^+ and Mg^{++}

sample	$(ratio)_A$	*E*
	Na^+ [a]	
3H(hRxF)	0.235	0.20
$3HS_2$(hFxR)	0.223	0.16
$3HS_3$(hFxR)	0.216	0.15
$3HS_3$(hRxF)	0.215	0.17
3H(rFxR)	0.254	0.22
$3HS_2$(rRxF)	0.250	0.22
$3HS_2$(rFxR)	0.255	0.20
$3HS_3$(rFxR)	0.262	0.21
$3HS_3$(rRxF)	0.247	0.19
3H(hRrF)	0.256	0.23
$3HS_2$(hRrF)	0.372	0.35
$3HS_2$(hFrR)	0.392	0.37
$3HS_3$(hRrF)	0.476	0.48
$3HS_3$(hFrR)	0.488	0.49
	Mg^{++} [b]	
$3HS_2$(hFxR)	0.200	0.13
$3HS_3$(hFxR)	0.188	0.12
$3HS_2$(rFxR)	0.254	0.20
$3HS_3$(rx)	0.229	0.17
$3HS_2$(hr)	0.372	0.35
$3HS_3$(hr)	0.461	0.46

[a] Table of the $(ratio)_A$ values and the FRET efficiencies of the three-way DNA junctions with and without bulge. Measurements have been performed at 4 °C in 90 mM TB buffer (pH 8.3) and 100 mM NaCl. The $(ratio)_A$ values have been determined according to eq 2, and the FRET efficiencies have been calculated from the $(ratio)_A$ values as described in the text. The error in the determination of the $(ratio)_A$ values is estimated to be ±0.005. The error of the *E* determination can be calculated from the errors given in the text for the ratios of the absorption coefficients, assuming that the labeling of the strands with fluorescein is 100%. [b] Table of the $(ratio)_A$ values and the FRET efficiencies of the three-way DNA junctions in the presence of 5 mM $MgCl_2$ at 4 °C. For some of the samples, the mean value of two vectors is given [e.g., the $(ratio)_A$ value for the $3HS_3$ (rx) molecule is the mean value of the molecules $3HS_3$ (rRxF) and $3HS_3$ (rFxR)]. See footnote a for the errors.

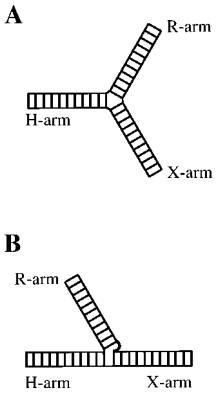

FIGURE 2: Schematics of the global structures for the 3H and $3HS_n$ molecules that are consistent with the FRET data. (A) The model for the DNA three-way junction with no unpaired nucleotides (3H) at the branch point is depicted as a symmetric Y-shaped molecule with approximately equal angles between the arms; there is no stacking interaction between the helical arms even at higher salt concentrations. (B) The unpaired adenine nucleotides in the r-strand at the branch point of the same molecule mediate a stacking between two of the arms of the molecule at higher salt concentrations and the structure becomes asymmetric. This structure represents our proposed stacking between the H and X arm; the R arm is inclined away from the bulge. The three helices may not be constrained to lie in a common plane, there may be a certain amount of flexibility in the structure, and the stacked helices may not be perfectly linear.

mM $MgCl_2$ (Figure 4). Other than minor differences of the FRET efficiency values due to the partial quenching of the donor fluorescence by Mg^{2+} (Clegg et al., 1992), the patterns of the FRET efficiencies for Na^+ and for Mg^{2+} are identical.

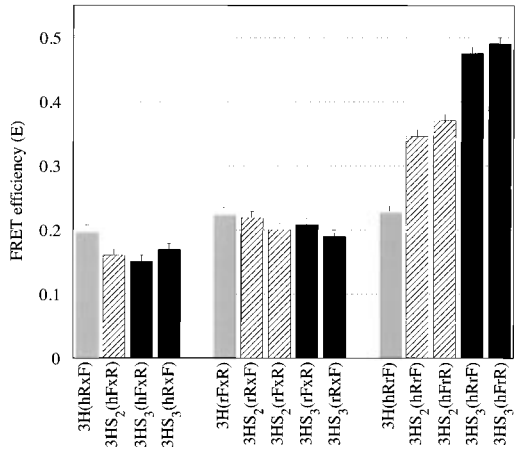

FIGURE 3: FRET efficiencies between fluorescein and TMRh covalently attached to the different 5′ ends of the 3H and $3HS_n$ molecules. The data are grouped by labeling-vector into three sets (HX, RX, and HR vectors). The number of unpaired nucleotides increases from left to right for every labeling vector. In each grouping the light shading, the inclined stripes and the black shading refer, respectively, to the 3H, the $3HS_2$, and the $3HS_3$ bulged molecules. The notation used in the figure can be illustrated by the example $3HS_n$(rRxF), which means that TMRh is attached to the 5′ end of the r-strand, and fluorescein to the 5′ end of the x-strand of the $3HS_n$ junction (three-way junction with n nucleotides in the bulge). All measurements were performed in 90 mM Tris borate buffer (pH 8.3), 100 mM NaCl at 4 °C.

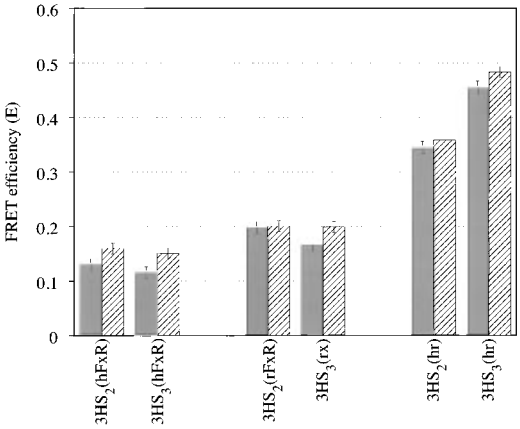

FIGURE 4: Comparison of the pattern of the FRET efficiency values for the $3HS_2$ and $3HS_3$ molecules in 100 mM NaCl (without added $MgCl_2$, gray bars) and in 5 mM $MgCl_2$ (without added NaCl, bars with inclined stripes). For some of the samples, the mean value of two vectors is given (e.g., the FRET efficiency for the $3HS_3$ (rx) molecule is the mean value of the molecules $3HS_3$ (rRxF) and $3HS_3$ (rFxR)).

DISCUSSION

Structural Implications of the FRET Efficiencies for the Geometry of the DNA Three-Way Junction at 100 mM NaCl. The salient features of the FRET results at 4 °C and the immediate direct structural interpretations can be summarized as follows.

(1) The FRET efficiencies for the 3H molecules (no bulge at the point of branch exchange) are about equal for all doubly labeled isomers (Figure 3). The FRET efficiency for the HX vector (∼0.20) is slightly lower than for the RX and the HR vectors (∼0.22). These data are consistent with an approximately symmetric trigonally shaped extended

conformation of the 3H molecule at higher salt concentrations (Welch et al., 1993; Duckett & Lilley, 1990). The FRET efficiencies are consistent with approximately equal angles between all pairs of arms.

(2) The FRET efficiencies for the HX vectors decrease from 0.2 to 0.15−0.16 as the number of unpaired adenine nucleotides increases (Figure 3), indicating an increase in the distances between the ends of the H- and X-arms. Welch et al. (1993) have shown by chemical probing of junctions with identical sequences at the branching region that at higher ionic strength the presence of unpaired bases at the point of branch exchange mediates a protection of the base pair faces between the H and the X arms. This was interpreted as colinear stacking of the two arms at the branch point (Welch et al., 1993). The decrease in the FRET efficiencies are compatible with a concerted movement of the X and R arms in order to stack coaxially at the branch point, but it is not possible to conclude from only the FRET efficiencies or from only the comparative gel electrophoresis assays, whether the arms actually stack.

(3) The FRET efficiencies for the RX vector change only slightly, from 0.22 to 0.19−0.20, as the number of unpaired nucleotides is varied, indicating only a small increase in the distance between the ends of the R and X arms. The *E* values are consistently slightly higher for the RX isomers compared to the HX isomers.

(4) The FRET efficiencies for the HR vector increase strongly from 0.23 (3H molecule) to about 0.50 ($3HS_3$ molecule) as the number of adenines in the bulges increases. This clearly indicates that the distance between the ends of the R and H arms is considerably reduced as the number of adenine bulges increases and that this reduction occurs progressively as the size of the bulge increases.

The global geometrical model that emerges from these FRET results is summarized in Figure 2. The symmetrical trigonal structure that is present in the absence of unpaired nucleotides (Figure 2A) becomes asymmetric in the presence of a bulge (Figure 2B). As the number of nucleotides in the bulge increases, the angle between two of the arms (the R and H arms) becomes significantly smaller and the angles between the other two pairs of arms (the RX vector and the HX vector) increase. As mentioned in the last paragraphs, two of the arms may actually form a quasi-continuous helix by stacking on each other. The third arm is inclined away from the bulge, forming a rather acute angle with its other neighboring arm. The inclination of the third arm to the quasi-continuous helix is intuitively what one expects from steric considerations; the strands at the end (at the junction) of the "unstacked" arm can more easily span the distances between the connecting nucleotides in the two stacked arms with less steric constraint if bulged nucleotides are present. The direction of inclination of the unstacked arm is also the direction relative to the bulge that has been proposed from comparative gel electrophoresis experiments (Welch et al., 1993, 1995) and from NMR studies (Leontis et al., 1993; Rosen & Patel, 1993b). Provided that the electrostatic repulsion of the backbone phosphates at the branch point is sufficiently suppressed by additional salt, the steric constraints and stacking interactions seem to control the global folding pattern of the molecule. Our FRET experiments show clearly that not only Mg^{2+} but also Na^+ is able to mediate the folding of the three-way DNA junction; this agrees with previous studies using other experimental methods (Leontis et al., 1991; Rosen & Patel, 1993a; Welch et al., 1995).

Asymmetry of the Sides of Branched Junctions May Lead to a Nonplanar Structure of the 3H. Three-way junctions have a major- and a minor-groove side at the point of branch exchange. This is a simple consequence of the continuity of the strands at the point of branch exchange as they pass from one arm to a neighboring arm (von Kitzing et al., 1990). Although our FRET results on the three-way DNA junction without a bulge are consistent with a triangular arrangement of the arms, where the angles between the arms are approximately equal, the structure is not constrained to be planar. Due to the asymmetry of the minor- and the major-groove sides of the molecule, it is likely that the structure has a pyramidal geometry (see also the discussion of the dye−dye distances below). Our results corroborate our interpretation of earlier comparative gel electrophoresis experiments on similar 3H junctions (Duckett & Lilley, 1990); in this earlier work it was found that no arms of the 3H three-way junctions without a bulge undergo coaxial stacking. This is supported by simple model building which shows that stacking of two of the arms in a three-way junction without a bulge would require significant distortions of the helix at the end of the third strand at the exchange point (see also discussion in the last paragraph), which might be expected to significantly lower the thermal stability of the three-way junction. In this respect, we note here that we have no evidence from the fluorescence intensity melting curves of a major stabilization, or destabilization, of the junctions without a bulge compared with those junction molecules with a bulge; this is discussed further in the following paper in this issue (Stühmeier et al., 1997).

Structural Aspects of the Three-Way DNA Junction with Bulge. The angle of inclination of the third arm relative to the quasi-continuous helix formed by the two-arm stacking of the three-way junction with a bulge with two pyrimidines has been estimated previously to be 80−90° (Leontis et al., 1994), leading essentially to a T structure. This value is based on estimates (from NMR measurements) of the helical axes of six base-pair helical arms by averaging the orientations of the few base pairs in the arms. Our FRET results indicate that the inclination of the third arm toward the quasi-continuous helix axis is more pronounced than this, at least for our molecules, especially when three adenine bases are in the bulge. The strongest, and most direct, evidence for this is the large difference between the FRET efficiencies for the RX and the HR vectors; this pronounced difference between the two vectors definitely excludes an approximate T structure, especially for the $3HS_3$ molecules. The FRET data, which are sensitive especially to changes in the long-range distances between the ends of the arms, corroborate the interpretation of electrophoresis measurements using a similar series of molecules with different combinations of long and short arms and the same central nucleotide sequence (Welch et al., 1993, 1995).

Direct evidence for stacking between two arms in the presence of a 2- or 3-nucleotide bulge comes from previous experiments showing that faces of the thymine nucleotides at the point of branch exchange of the three-way junction with bulge are not chemically reactive (Leontis et al., 1993; Welch et al., 1993) and from NMR experiments (Leontis et al., 1995; Overmars et al., 1996; Rosen et al., 1992; Rosen & Patel, 1993b). The stacking geometry at the branch point

may be quite different from that found in a normal B-DNA helix, but the extent of stacking is apparently sufficient so that the faces of the nucleotides belonging to these two helices are shielded from attack by small reactive chemicals. If the two arms are stacked in a *linear* continuous helix, the axis for the third arm would always define a planar configuration for the three arms (as shown in Figure 2) and this would allow the calculation of the third angle; but the folded structure is not restrained to be planar if the two stacked arms are not really colinear.

Approximate Distances between the Donor and Acceptor Molecules from the FRET Efficiencies. We can make approximate calculations of the distances between the two dyes using simple geometrical models and assumptions about the R_0 values (see Materials and Methods). We emphasize that our conclusions concerning the structure do not depend on these quantitative estimates; but it is important to show that the calculated distances are reasonable considering the dimensions of our helical arms. The positions and interactions of the donor and acceptor molecules with the nucleic acid duplex, and their effect on FRET measurements, have been reported recently (Clegg et al., 1994; Vámosi et al., 1996). We have measured R_0 to be 50 Å for the conditions of the experiments. The FRET efficiencies of the open structure are approximately 0.2 which corresponds to $R = 1.25R_0$ and leads to an expected distance between the donor and acceptor of ~63 Å. If we make the approximation that the arms are 46 Å long[6] from the middle of the branch point to the ends of the helices, this corresponds to a trigonal pyramid with angles of 86° with edges 46 Å long (that is, the open form of the three-way junction without a bulge would not be planar). The lowest FRET efficiency of the folded form is 0.15. This corresponds to a distance of 67 Å, which is approximately the length of two 34 Å colinear helices. The highest FRET efficiency value is 0.5 (for the $3HS_3$ bulged junction) which represents a distance of 50 Å (if $R_0 = 50$ Å) and corresponds to an angle of 66° between two linear 45 Å long arms.

These calculations are very approximate and correspond to only an ensemble-averaged structure; they do not take into account the full three-dimensional structure of the junction or the possibility of flexibility of the arms leading to a distribution of the relative arm orientations, and they can also be in error due to uncertainties in R_0 (especially κ^2) values. However, it is important that the approximate dimensions of the three-way junction are reflected in the FRET efficiencies that we measure. Perhaps most importantly, these estimates show that our FRET results are in fact in reasonable agreement with a model where there are stacking interactions between two of the arms, and an inclination of approximately 60° between the third arm and the quasi-continuous helical axis for the model of the $3HS_3$ probe in Figure 2B.

[6] The value of 46 Å is calculated as follows. The lengths of the 10 bp arms are assumed to be 34 Å long. We arrange the helices onto a planar surface such that the connecting points of the ends of the helices at the center of the branch point form a equilateral triangle. Then the axial distance from the outer end of any 10 bp helix to the center of this triangle is 43.5 Å. The fluorescein molecule is extended from the helix, and the TMRh is tucked into the helix. We estimate that this gives an average distance of the dyes from the ends of the helices of approximately 2.5 Å. This corresponds to a value of 46 Å for the length of an edge.

Global Geometry of Bulged Three-Way DNA Junctions Is Similar in the Presence of Sufficient Na^+ or Mg^{++}. The pattern of the FRET efficiencies for the $3HS_2$ and the $3HS_3$ molecules are identical in 100 mM NaCl (no $MgCl_2$) and in 5 mM $MgCl_2$ (no added NaCl) (see Figure 4). This indicates that NaCl alone can mediate complete folding of the three-way junction with two or three adenine nucleotides in the bulge and that the global folded structure is similar to that produced by Mg^{2+} ions. The necessary NaCl concentration for the complete folding is lower than that required for the complete folding of the four-way junction (Clegg et al., 1994). The ability of NaCl to induce folding is consistent with Rosen and Patel (1993a), who report that there is no additional influence of Mg^{2+} ions on the structure of three-way DNA junctions at higher concentrations of NaCl; although, it should be noted that their junction adopted a stereochemically distinct alternative stacking conformer. This is also consistent with another recent NMR study (Overmars et al., 1996) and with comparative gel electrophoresis experiments (Welch et al., 1995) which show similar folded structures in the presence of sufficient NaCl (>30 mM), as in 1 mM $MgCl_2$.

It was not possible to determine reliable and reproducible FRET efficiencies for our three-way junction molecules with 10 bp arms in the absence of additional sodium or magnesium ions (e.g., if [Na+] < 30 mM). At very low salt conditions, the anisotropy values of TMRh and the FRET efficiencies clearly indicate that the molecules are not completely double stranded, even at 4 °C. It was difficult to reproduce spectroscopic measurements at these conditions over an extended time, indicating slow kinetic processes under these conditions (data not shown). This is probably a result of partial melting of the junction molecules with such short arms (10 base pairs) at very low salt conditions. Reliable and reproducible spectroscopic measurements can however be made at sodium chloride concentrations of at least 40 mM. In addition to the possible instability of the equilibrium structures at low salt, it is known that the individual steps of base-pair formation become slower as the ionic strength of the solution is lowered (Anshelevich et al., 1984; Craig et al., 1971; Pörschke & Eigen, 1971). We have found that the presence of a multiarm branch, such as a four-way junction, in a DNA duplex leads to much slower hybridization kinetics than found for DNA duplexes with no irregularities in the helical structures (G. Vámosi et al., unpublished data); although we have not studied this phenomenon for the three-way junction in detail, preliminary results indicate that this slow kinetic effect is also present with the three way structures.

Flexibility at the Branch Point. Our measurements do not address the question of flexibility of the junctions but determine the overall tendency of the $3HS_n$ molecules to fold in a particular global conformation. Our proposed global folding pattern of the arms when a bulge is introduced (Figure 3) shows distinct differences between the end-to-end distances of different pairs of arms similar to another recent time-resolved FRET study on three-way junctions with bulges; these authors have interpreted their data in terms of distribution models that emphasize the flexible nature of the branched structures (Yang & Millar, 1996). A certain amount of flexibility is to be expected; in the presence of a distribution of conformations, steady-state FRET measurements will reflect a weighted statistical average over the

ensemble. In both cases, differences between the average inclinations between neighboring arms are evident.

A number of experimental differences complicate the comparison of our data with those of Yang (Yang & Millar, 1996). Their measurements were carried out at 20 °C, and their junctions were constructed from eight base-pair arms with AT base pairs at the free labeled ends of all three arms. It could be that the $3HS_2$ junctions they investigated were not fully stable under the conditions of their experiment. The authors reported the presence of a 1−20% fraction of incomplete three-way junctions which they attributed possibly to unstable junctions (Yang & Millar, 1996). To diminish the propensity for fraying at the ends, we have used two CG base pairs at the end of each 10 base-pair helix; in addition we measured the FRET at 4 °C, far below the melting temperature of the duplex structure. How much these thermodynamic and spectroscopic factors influence the interpretations of FRET experiments in terms of molecular flexibilities of the junction structure or how much the molecular structures will be influenced themselves remains to be seen; this will undoubtedly be a major issue of future investigations into the structures of branched DNA and RNA structures.

Are There Different Global Conformations Depending on the Sequence? The overall structures of the $3HS_2$ molecules proposed by Yang and Millar (1996), who studied the influence of CC, GG, AA, and TT bulges on the global structure of the three-way junction, are quite different from that proposed here, or from those found in the NMR structures or from our structure. In the model of Yang et al., the two helical arms that are most colinear both share the strand with the bulge; these authors do not say that the helices are actually colinear, and because the arms are expected to have flexibility according to their model, the structure they present is an average structure. Coaxial stacking has been convincingly demonstrated in each of the NMR structures of three-way junctions (Altona et al., 1996; Leontis et al., 1994; Ouporov & Leontis, 1995; Rosen et al., 1992) and is also consistent with the protection of bases against chemical attack in the folded conformation of our $3HS_n$ junctions (Welch et al., 1993). However, in these structures, the bulge-containing strand is not shared between the coaxially stacked helices; it would be very difficult to envision how uninterrupted stacking would be possible if the two arms containing the bulged nucleotides were stacked in an approximate B-DNA geometry. By contrast, if the strand with the bulged nucleotides is shared by one of the coaxially stacked arms and by the third arm, there is enough conformational tractability to accommodate the stacking without disrupting any of the helical structures at the branch point. This conclusion is in accord with molecular model building of three-way junctions; it is not possible for two arms of a 3H molecule to stack in a B-like structure; and accommodate the third arm without significantly distrupting the base-pair structure of this third arm at the branch point. This does not mean that stacking interactions between two arms cannot take place, but that the base stacking would probably be quite different from the normal B structure for 3H structures. If there are sequence differences in the stability of base stacking of base pairs in the vicinity of the branch point of three-way junctions, this could lead to different overall stereochemical arrangements of the arms at the junction and to different flexibilities of the whole structure.

CONCLUSIONS

In this study we have shown that there is a qualitative difference between the stereochemistry of the three-way junction molecules with and without bulges at the branch point. Whereas the FRET results are consistent with a symmetrical trigonal pyramidal orientation between the three arms in the absence of a bulge, the structure assumes an asymmetrical structure in the presence of bulged nucleotides in one of the arms, and the extent of asymmetry increases with increasing number of nucleotides in the bulge. The structure derived from the FRET studies of the three-way junctions with bulged nucleotides is consistent with a stacking between two of the arms at the branch point, and an inclined orientation of the third (nonstacked) arm to the other two (stacked) arms. One of the complementary strands of this third helical arm contains the strand that has the extra bulge nucleotides.

ACKNOWLEDGMENT

F.S. and R.M.C. thank G. Vámosi and C. Gohlke for communication of their data prior to publication and many valuable discussions and A. Zechel for technical assistance. We thank Reinhard Klement for help with molecular modeling of the three-way junctions and O. Holub and A. Zechel for reading the manuscript.

REFERENCES

Altona, C., Pikkemaat, J. A., & Overmars, F. J. J. (1996) *Curr. Opin. Struct. Biol. 6*, 305−316.
Anshelevich, V. V., Vologodskii, A. V., Lukashin, A. V., & Frank-Kamenetskii, M. D. (1984) *Biopolymers 23*, 39−58.
Beaucage, S. L., & Caruthers, M. H. (1981) *Tetrahedron Lett. 22*, 1859−1862.
Bennett, R. J., & West, S. C. (1995) *J. Mol. Biol. 252*, 213−226.
Bhattacharyya, A., & Lilley, D. M. J. (1989) *Nucleic Acids Res. 17*, 6821−6840.
Bhattacharyya, A., Murchie, A. I. H., & Lilley, D. M. J. (1990) *Nature 343*, 484−487.
Bhattacharyya, A., Murchie, A. I. H., von Kitzing, E., Diekmann, S., Kemper, B., & Lilley, D. M. J. (1991) *J. Mol. Biol. 221*, 1191−1207.
Bianchi, M. E., Beltrame, M., & Paonessa, G. (1989) *Science 243*, 1056−1059.
Bianchi, M. E., Falciola, L., Ferrari, S., & Lilley, D. M. J. (1992) *EMBO J. 11*, 1055−1063.
Clegg, R. M. (1992) *Methods Enzymol. 211*, 353−388.
Clegg, R. M. (1996) in *Fluorescence Imaging Spectroscopy and Microscopy* (Wang, X. F., & Herman, B., Eds.) pp 179−252, John Wiley & Sons, Inc., New York.
Clegg, R. M., Murchie, A. I. H., Zechel, A., Carlberg, C., Diekmann, S., & Lilley, D. M. J. (1992) *Biochemistry 31*, 4846−4856.
Clegg, R. M., Murchie, A. I. H., Zechel, A., & Lilley, D. M. J. (1993) *Proc. Natl. Acad. Sci. U.S.A. 90*, 2994−2998.
Clegg, R. M., Murchie, A. I. H., & Lilley, D. M. J. (1994) *Biophys. J. 66*, 99−109.
Connolly, B. A. (1987) *Nucleic Acids Res. 15*, 3131−3139.
Cooper, J. P., & Hagerman, P. J. (1990) *Biochemistry 29*, 9261−9268.
Craig, M. E., Crothers, D. M., & Doty, P. (1971) *J. Mol. Biol. 62*, 383−401.
Dale, R. E., & Eisinger, J. (1974) *Biopolymers 13*, 1573−1605.
Demas, J. N., & Crosby, G. A. (1971) *J. Phys. Chem. 75*, 991−1024.
Duckett, D. R., & Lilley, D. M. (1990) *EMBO J. 9*, 1659−1664.

Duckett, D. R., Murchie, A. I. H., Diekmann, S., von Kitzing, E., Kemper, B., & Lilley, D. M. J. (1988) *Cell 55*, 79−89.
Duckett, D. R., Murchie, A. I. H., Clegg, R. M., Zechel, A., von Kitzing, E., Diekmann, S., & Lilley, D. M. J. (1990) in *Human Genome Initiative & DNA Recombination* (Sarma, R. H., & Sarma, M. H., Eds.) pp 157−181, Adenine Press, Guilderland, NY.
Duckett, D. R., Murchie, A. I. H., Bhattacharyya, A., Clegg, R. M., Diekmann, S., von Kitzing, E., & Lilley, D. M. J. (1992) *Eur. J. Biochem. 207*, 285−295.
Duckett, D. R., Giraud Panis, M.-E., & Lilley, D. M. J. (1995a) *J. Mol. Biol. 246*, 95−107.
Duckett, D. R., Murchie, A. I. H., & Lilley, D. M. J. (1995b) *Cell 83*, 1027−1036.
Eggleston, A. K., & West, S. C. (1996) *Trends Genet. 12*, 20−26.
Eis, P. S., & Millar, D. P. (1993) *Biochemistry 32*, 13852−13860.
Förster, T. (1948) *Ann. Phys. 2*, 55−75.
Förster, T. (1949) *Z. Naturforsch. 4a*, 321−327.
Gohlke, C., Murchie, A. I. H., Lilley, D. M. J., & Clegg, R. M. (1994) *Proc. Natl. Acad. Sci. U.S.A. 91*, 11660−11664.
Jablonski, A. (1957) *Acta Phys. Pol. 16*, 471−479.
Jares-Erijman, E. A., & Jovin, T. M. (1996) *J. Mol. Biol. 257*, 596−617.
Lakowicz, J. R. (1983) *Principles of fluorescence Spectroscopy*, Plenum Press, New York.
Leontis, N. B., Kwok, W., & Newman, J. S. (1991) *Nucleic Acids Res. 19*, 759−766.
Leontis, N. B., Hills, M. T., Piotto, M., Malhotra, A., Nussbaum, J., & Gorenstein, D. G. (1993) *J. Biomol. Struct. Dyn. 11*, 215−223.
Leontis, N. B., Hills, M. T., Piotto, M., Ouporov, I. V., Malhotra, A., & Gorenstein, D. G. (1994) *Biophys. J. 68*, 251−265.
Leontis, N. B., Hills, M. T., Piotto, M., Ouporov, I. V., Malhotra, A., & Gorenstein, D. G. (1995) *Biophys. J. 68*, 251−265.
Lilley, D. M. J., & Clegg, R. M. (1993a) *Q. Rev. Biophys. 26*, 131−175.
Lilley, D. M. J., & Clegg, R. M. (1993b) *Annu. Rev. Biophys. Biomol. Struct. 22*, 299−328.
Lilley, D. M. J., Clegg, R. M., Diekmann, S., Seeman, N. C., Kitzing, E. v., & Hagerman, P. M. (1995) *Eur. J. Biochem. 239*, 1−2.
Millar, D. P. (1996) *Curr. Opin. Struct. Biol. 6*, 322−326.
Murchie, A. I. H., Clegg, R. M., von Kitzing, E., Duckett, D. R., Dieckmann, S., & Lilley, D. M. J. (1989) *Nature 341*, 763−766.
Nickel, B. (1989) *J. Lumin. 44*, 1−18.
Ouporov, I. V., & Leontis, N. B. (1995) *Biophys. J. 68*, 266−274.
Overmars, F. J. J., Pikkemaat, J. A., Elst, H. v. d., Boom, J. H. v., & Altona, C. (1996) *J. Mol. Biol. 255*, 702−713.
Parsons, C. A., Stasiak, A., Bennett, R. J., & West, S. C. (1995) *Nature 374*, 375−378.
Pöhler, J. R. G., Duckett, D. R., & Lilley, D. M. J. (1994) *J. Mol. Biol. 238*, 62−74.
Pöhler, J. R. G., Giraud-Panis, M.-J. E., & Lilley, D. M. J. (1996) *J. Mol. Biol. 260*, 678−696.
Pörschke, D., & Eigen, M. (1971) *J. Mol. Biol. 62*, 361−381.
Rosen, M. A., & Patel, D. J. (1993a) *Biochemistry 32*, 6563−6575.
Rosen, M. A., & Patel, D. J. (1993b) *Biochemistry 32*, 6576−6587.
Rosen, M. A., Live, D., & Patel, D. J. (1992) *Biochemistry 31*, 4004−4014.
Seeman, N. C., & Kallenbach, N. R. (1994) *Annual Review of Biophysics & Biomolecular Structure*, pp 53−86, Annual Reviews Inc., Palo Alto.
Sinha, N. D., Biernat, J., McManus, J., & Koster, H. (1984) *Nucleic Acids Res. 12*, 4539−4557.
Stühmeier, F., Lilley, D. M. J., & Clegg, R. M. (1997) *Biochemistry 36*, 13539−13551.
Teo, S. H., Grasser, K. D., Hardman, C. H., Broadhurst, R. W., Laue, E. D., & Thomas, J. O. (1995) *EMBO J. 14*, 3844−3853.
Tuschl, T., Gohlke, C., Jovin, T. M., Westhof, E., & Eckstein, F. (1994) *Science 266*, 785−789.
Vámosi, G., Gohlke, C., & Clegg, R. M. (1996) *Biophys. J. 71*, 972−994.
Van Der Meer, B. W., Coker, G., III, & Chen, S.-Y. S. (1994) *Reson. Energy Transfer*, VCH Publishers, Inc., New York.
von Kitzing, E., Lilley, D. M. J., & Diekmann, S. (1990) *Nucleic Acids Res. 18*, 2671−2683.
Welch, J. B., Duckett, D. R., & Lilley, D. M. (1993) *Nucleic Acids Res. 21*, 4548−4555.
Welch, J. B., Walter, F., & Lilley, D. M. (1995) *Journal of Molecular Biology 251*, 507−519.
White, M. F., & Lilley, D. M. J. (1996) *J. Mol. Biol. 266*, 122−134.
Yang, M., & Millar, D. P. (1996) *Biochemistry 35*, 7959−7967.
Zhong, M., Rashes, M. S., Leontis, N. B., & Kallenbach, N. R. (1994) *Biochemistry 33*, 3660−3667.

BI9702445